

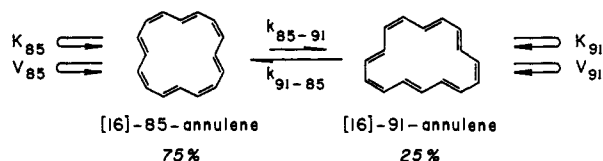
## The Radical Anion and the Dianion of [16]Annulene

J. F. M. Oth,\* H. Baumann, J.-M. Gilles, and G. Schröder

Contribution from the Laboratory for Organic Chemistry,  
Swiss Federal Institute of Technology, 8006 Zürich, Switzerland,  
and the Institute for Organic Chemistry, Karlsruhe University,  
7500 Karlsruhe 1, West Germany. Received July 19, 1971

**Abstract:** In aprotic solvents [16]annulene can be reduced electrochemically or by alkali metals to its radical anion and its dianion. These two species have been studied by different spectroscopic methods and information concerning their structure and their stability has been obtained. The esr spectrum of the radical anion is reported. Its interpretation, based on symmetry and HMO (with variable  $\beta$ ) considerations, has allowed us to establish unambiguously the structure of this species and to conclude which of the two nonbonding MO's is in fact occupied by the unpaired electron. The structure of the dianion could be deduced from nmr studies. The nmr spectrum of this aromatic species is very informative; the diamagnetism associated with the delocalized  $18\pi$ -electron system is clearly demonstrated by the fact that the resonance signal of the inner protons appears at extremely high field ( $\tau$  18.17). The nmr spectrum of the dianion is temperature independent, unlike that of the parent [16]annulene molecule and that of the isoelectronic [18]annulene. This difference in dynamic behavior is discussed. Uv-visible absorption spectra of the two species ( $R^{\cdot-}$  and  $R^{2-}$ ) are reported; they indicate that both species are most probably planar. The thermal stability of the dianion is found to be very great in contrast to that of the parent [16]annulene molecule.

By nmr spectroscopy studies<sup>1</sup> [16]annulene, synthesized by Sondheimer and Gaoni<sup>2</sup> and by Schröder and Oth,<sup>3</sup> has been shown to exist in solution as a dynamic equilibrium between two interconverting configurations,



each exhibiting single and double bond alternation but differing from the other by the number and sequence of cis and trans double bonds.<sup>4</sup> Each of these configurations undergoes conformational mobility ( $K_{85}$  and  $K_{91}$ ) and fast bond shift ( $V_{85}$  and  $V_{91}$ ). These isodynamic processes<sup>5</sup> are responsible for the fact that the inner and outer protons in each structure are indistinguishable by nmr spectroscopy above  $-80^\circ$  (at 60 MHz).<sup>6</sup> Furthermore, the isomerization rates  $k_{85 \rightarrow 91}$  and  $k_{91 \rightarrow 85}$  are

large enough above  $-60^\circ$  to bring about coalescence of the nmr lines of the two configurations.<sup>1</sup>

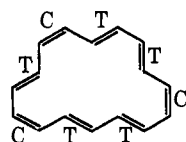
We were interested in studying how the relative energies, the geometries, and the dynamic behavior of these configurations would be affected by the introduction of one and of two excess electrons into their  $\pi$  systems. In particular the dianion(s) of [16]annulene possessing  $(4n + 2)$   $\pi$  electrons may be expected to be quite stable, to show no bond alternation, and to exhibit a dynamic behavior (which could cause nmr equivalence of the inner and outer protons) much slower than that of the neutral molecules. Such a dynamic behavior is in fact observed in the case of [18]annulene.<sup>7</sup>

We report here the spectroscopic evidence that we have obtained for the existence and the stability of the radical anion  $R^{\cdot-}$  (uv-visible and esr spectra) and of the dianion  $R^{2-}$  (uv-visible and nmr spectra) of [16]annulene. The configuration, the geometry, and the relative stability of these species are discussed.

## I. Theoretical Considerations

The main problems that we had to solve were to establish the configurations of the radical anion and of the dianion and to find out if these species do or do not show bond alternation and are or are not planar. Answers to these questions could be obtained by comparison of the experimental facts (the esr spectrum in the case of  $R^{\cdot-}$ , the nmr and uv-visible spectra in the case of  $R^{2-}$ ) with the theoretical results based on symmetry considerations and MO computations.

**A. The Variable  $\beta$  Hückel Approximation.** As is well known, the successes of Hückel molecular orbital (HMO) calculations are, to a great extent, due to the fact that they take into account the "topology" of the molecular skeleton.<sup>8,9</sup> In cases where the symmetry of the correct electronic Hamiltonian is governed only by



sequence	C T C T T C T T
smallest binary no.	0 1 0 1 1 0 1 1
denary no.	$2^6 + 2^4 + 2^3 + 2 + 1 = 91$

Hence, this structure is identified as the [16]-91-annulene.

(5) For the definition of an isodynamic process, see: S. L. Altman, *Proc. Roy. Soc., Ser. A*, **298**, 184 (1967).

(6) The exchange mechanism by which all the protons of [16]annulene become equivalent in nmr spectroscopy is explained in ref 3 ([16]-85-annulene) and in ref 1.

(7) Y. Gaoni, A. Melera, F. Sondheimer, and R. Wolovsky, *Proc. Chem. Soc.*, 397 (1964); F. Sondheimer, *Proc. Roy. Soc., Ser. A*, **297**, 173 (1967).

(8) K. Ruedenberg, *J. Chem. Phys.*, **34**, 1884 (1961).

(9) U. Wild, J. Keller, and Hs. H. Günthard, *Theor. Chim. Acta*, **14**, 383 (1969).

the topology of the molecule (this is the case for condensed aromatic molecules) it is often sufficient to use the original version of Hückel theory in which all coulomb integrals ( $\alpha$ ) on the one hand, and all resonance integrals ( $\beta$ ) on the other, are assumed to be equal.

However, in the case of an annulene of a given size, one can imagine many structures which share the common topology of a simple ring. It is thus necessary to relax somewhat the drastic assumption of simple Hückel theory in order that the approximate one-electron Hamiltonian has a more correct symmetry. For example, the constant  $\beta$  approximation is justified for benzene but not for cyclooctatetraene in which cis double bonds and gauche single bonds alternate.<sup>10</sup> Neither can it be used for [18]annulene [a  $(4n + 2)$   $\pi$ -electron system] if one wants to allow for the  $D_{6h}$  symmetry of this molecule.<sup>11,12</sup>

Numerous applications to neutral molecules (mostly alternant conjugated hydrocarbons) in which the resonance integrals  $\beta$  are varied as a function of bond length according to semiempirical relationships<sup>13-15</sup> have been reported. However, in the case of ions, Hückel calculations have mostly been confined to the constant  $\beta$  approximation.<sup>16</sup> Yet one has to expect that for such species HMO computations in the variable  $\beta$  approximation will give valuable results not only as far as the symmetry is concerned but also as regards the qualitative effects of structural changes on spectroscopic properties.

One of our aims has thus been to identify the structures of the [16]annulene radical anion  $R^{\cdot-}$  and dianion  $R^{2-}$  by comparing their spectroscopic properties with those calculated by the variable  $\beta$  approximation. In this work we have considered neither the variation of coulomb integrals nor the introduction of long-range interactions since, as will be shown in the Discussion, variation of  $\beta$  alone is sufficient to solve the structure problems.

**B. The Different Perimeters Investigated.** As noted in the introductory statement, among the many possible configurations of a [16]annulene, two are known to exist in measurable amounts in solution. In the crystal, however, [16]annulene exists only in the 85 configuration,<sup>4</sup> as was shown by X-ray crystallography. In this configuration the molecule has  $S_4$  symmetry and consists essentially of four planar butadiene residues linked together by four gauche single bonds with torsion angles of  $40^\circ$ .<sup>17,18</sup> The geometry of the less abundant isomer, [16]-91-annulene,<sup>4</sup> is not known exactly since this isomer has not been isolated in crystalline form. Were it not for the severe interactions between

the inner hydrogens, [16]-91-annulene could be planar (all bond angles would be equal or close to  $120^\circ$ ) and have  $C_8$  symmetry ( $C_{2v}$  symmetry if there were no bond alternation).

The dianion of [16]annulene should be aromatic according to Hückel's rule.<sup>13</sup> This implies that the 18  $\pi$  electrons are delocalized and that the dianion is nearly planar and shows no bond alternation. One might assume that the framework of the dianion could derive from the framework of either one or both of the observed isomers of the neutral molecule (e.g., that, for strain reason, the 91 configuration might be preferred).

The radical anion could also have its 17  $\pi$  electrons delocalized, thus showing no bond alternation and tending toward a planar geometry. Such a structure of the radical anion would imply, in the simple Hückel theory (i.e., all  $\beta$  values are equal), that the unpaired electron occupies one of the two degenerate nonbonding MO's and thus would violate the Jahn-Teller theorem.<sup>19</sup> However, since a planar [16]annulene radical anion (even assuming all bonds equal in length) will necessarily take up a geometry with a lower symmetry than that implied by the simple Hückel approximation ( $D_{16h}$ ),<sup>20</sup> the degeneracy (in symmetry) of the two nonbonding Hückel MO's may not exist. One might again here assume that the framework of the radical anion will derive from that of one or both of the observed isomers ([16]-85- and [16]-91-annulene).

Following this assumption, we have investigated five different Hückel perimeters; these and the corresponding possible true geometries are represented in Table I. The table gives also, for each perimeter, the symmetry, the degeneracy, and the coefficients of the two nonbonding MO's.<sup>21</sup> The first and second perimeters correspond to hypothetical molecules with equal and with alternant single and double bonds, respectively. One of the structures corresponding to the second perimeter is that of neutral [16]-91-annulene (planar). The third perimeter corresponds to the structure of neutral [16]-85-annulene and depends on three resonance integrals. The fourth describes a delocalized [16]-85 structure in which all the inner and outer C-C bonds form two sets of equivalent bonds. This situation prevails in [18]annulene and it corresponds, for instance, to a [16]-85-annulene structure of  $D_{4h}$  symmetry. Finally, the fifth perimeter describes a delocalized structure of [16]-91-annulene in which, once again, all the inner C-C bonds on the one hand, and all the outer ones on the other hand, are equivalent. The physical reason for adopting the bond length pattern of the last two perimeters has already been invoked to explain the bond pattern observed<sup>11</sup> in the planar [18]annulene. It results from the mutual repulsions of the inner hydrogen atoms in a quasiplanar delocalized structure. The repulsion energy is diminished to some extent by an opening of the adjacent CCC angles; this opening, in turn, changes the hybridization of the

(10) M. Traetteberg, *Acta Chem. Scand.*, **20**, 1724 (1966).

(11) J. Bregman, F. L. Hirschfeld, D. Rabinovich, and G. M. J. Schmidt, *Acta Crystallogr.*, **19**, 227 (1965).

(12) F. L. Hirschfeld and D. Rabinovich, *ibid.*, **19**, 235 (1965).

(13) L. Salem, "Molecular Orbital Theory of Conjugated Systems," W. A. Benjamin, New York, N. Y., 1966.

(14) H. C. Longuet-Higgins and L. Salem, *Proc. Roy. Soc., Ser. A*, **251**, 172 (1959).

(15) C. A. Coulson and A. Gotebiewski, *Proc. Phys. Soc.*, **78**, 1310 (1961).

(16) I. Bernal, P. H. Rieger, and G. K. Fraenkel, *J. Chem. Phys.*, **37**, 1489 (1962).

(17) G. S. D. King, *Union Carbide ERA Tech. Memorandum*, No. 102, (1968); S. M. Johnson, I. C. Paul, and G. S. D. King, *J. Chem. Soc. B*, 643 (1970).

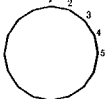
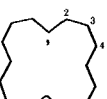
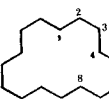
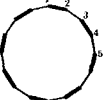
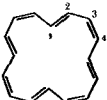
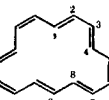
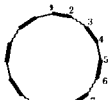
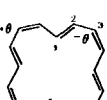
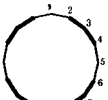
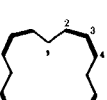
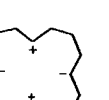
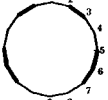
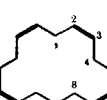
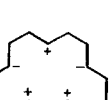
(18) Such a structure (i.e., 85 configuration and nonplanar conformation with  $S_4$  symmetry) was proposed prior to the X-ray studies in order to explain the nmr spectrum of [16]annulene as observed at  $-110^\circ$  (cf. ref 3).

(19) H. A. Jahn and E. Teller, *Proc. Roy. Soc., Ser. A*, **161**, 220 (1937).

(20) In a structure with  $D_{16h}$  symmetry (i.e., planar with all bonds cis, all bond lengths and all bond angles equal) the bond angle strain would be very high; planar structures with cis and trans bonds must be less strained.

(21) The expression "nonbonding MO's" refers to MO's which are correlated with the nonbonding MO's of the  $D_{16h}$  simple Hückel perimeter.

**Table I.** Hückel Perimeters Investigated (Variable  $\beta$  Approximation); Corresponding True Geometries; Symmetry, Degeneracy, and AO Coefficients for the Two Nonbonding MO's

Hückel perimeters	Some corresponding geometries	Symmetry	Degeneracy	Nonbonding MO's	Atomic orbital coefficients
 $D_{16h}$	 $D_{4h}$	 $C_{2v}$	$e_{4u}$  $e_{4u}$	Degenerate	$\frac{1}{2\sqrt{2}} \cos\left(r \frac{\pi}{2}\right)$ $\frac{1}{2\sqrt{2}} \sin\left(r \frac{\pi}{2}\right)$ $r = 1, 2, 3 \dots 16$
 $D_{8h}$	 $C_{4h}$	 $C_s$	$b_{1u}$  $b_{2u}$	Not degenerate	$\frac{1}{2\sqrt{2}} \cos\left(r \frac{\pi}{2} + \frac{\pi}{4}\right)$ $\frac{1}{2\sqrt{2}} \sin\left(r \frac{\pi}{2} + \frac{\pi}{4}\right)$ $r = 1, 2, 3 \dots 16$
 $D_{4h}$	 $S_4$		$a_{1u}$  $a_{2u}$	Not degenerate	$\frac{1}{2\sqrt{2}} \sin\left(\frac{\pi}{4} + \frac{\phi}{2} - p \frac{\pi}{2}\right) (-1)^{r-1}$ with $\tan \phi = (\beta_2 - \beta_3)/2\beta_1$ $p$ parity of $[r/2]$ $\frac{1}{2\sqrt{2}} \sin\left(\frac{\pi}{4} + \frac{\phi}{2} - p \frac{\pi}{2}\right)$ $p = 0$ for $r = 1, 4, 5, 8, 9, 12, 13, 16$ $p = 1$ for $r = 2, 3, 6, 7, 10, 11, 14, 15$
 $D_{4h}$	 $D_{4h}$	 $D_{2d}$	$a_{1u}$  $a_{2u}$	Not degenerate for symmetry Degenerate for energy	$\frac{1}{2\sqrt{2}} \cos\left(r \frac{\pi}{2}\right)$ $\frac{1}{2} \sin\left(r \frac{\pi}{2}\right) \cos\left(\psi - p \frac{\pi}{2}\right)$ with $\tan \psi = \beta_1/\beta_2$ , $p$ as above
 $C_{2v}$	 $C_{2v}$	 $C_g$	$a_2$  $b_2$	Not degenerate for symmetry Degenerate for energy	$\begin{cases} 0 & \text{if } q \text{ even} \\ \pm \frac{1}{2} \cos\left(\chi + p \frac{\pi}{2}\right) & \text{if } q > 0, - \text{ if } q < 0 \end{cases}$ $\begin{cases} \sin \chi / \sqrt{1 + 6 \cos^2 \chi} & \text{for } q = 0 \\ \cos \chi \cos\left(q \frac{\pi}{2}\right) / \sqrt{1 + 6 \cos^2 \chi} & \text{for } q \neq 0 \end{cases}$ with $\tan \chi = \beta_2/\beta_1$ , $q = r - 1$ for $r \leq 9$ $q = r - 17$ for $r > 9$ $q = -7, -6, \dots, -1, 0, \dots, 7, 8$

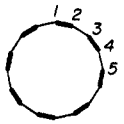
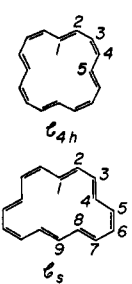
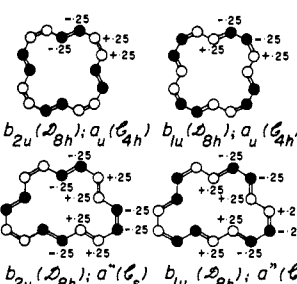
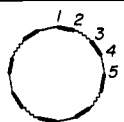
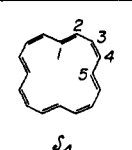
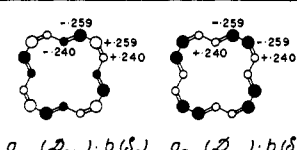
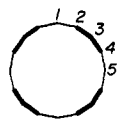
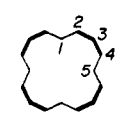
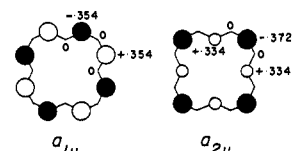
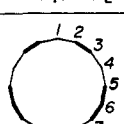
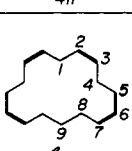
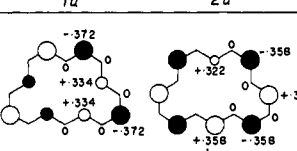
Hückel perimeters	Corresponding geometries	Atomic orbital coeff and energies of the "non bonding" MO's for the $\beta$ values indicated
<p>• 2</p>  <p><math>D_{8h}</math> (<math>-\beta_1, -\beta_2</math>)</p>	 <p><math>C_{4h}</math> <math>C_s</math></p>	 <p><math>b_{2u}(D_{8h}); a_u(C_{4h})</math> <math>b_{1u}(D_{8h}); a_u(C_{4h})</math> <math>\beta_1 \neq \beta_2</math> <math>b_{2u}(D_{8h}); a^-(C_s)</math> <math>b_{1u}(D_{8h}); a^-(C_s)</math> <math>E(b_{2u}) = 0.25\beta</math> <math>E(b_{1u}) = -0.25\beta</math></p>
<p>• 3</p>  <p><math>D_{4h}</math> (<math>-\beta_1, -\beta_2, -\beta_3</math>)</p>	 <p><math>D_{4h}</math></p>	 <p><math>a_{1u}(D_{4h}); b(D_{4h})</math> <math>a_{2u}(D_{4h}); b(D_{4h})</math> <math>\beta_1 = 1</math> <math>\beta_2 = .6</math> <math>\beta_3 = .75</math> <math>E(a_{1u}) = 0.328\beta</math> <math>E(a_{2u}) = -0.328\beta</math></p>
<p>• 4</p>  <p><math>D_{4h}</math> (<math>-\beta_1, -\beta_2</math>)</p>	 <p><math>D_{4h}</math></p>	 <p><math>a_{1u}</math> <math>a_{2u}</math> <math>\beta_1 = 1</math> <math>\beta_2 = .9</math> <math>E(a_{1u}) = 0</math> <math>E(a_{2u}) = 0</math></p>
<p>• 5</p>  <p><math>C_{2v}</math> (<math>-\beta_1, -\beta_2</math>)</p>	 <p><math>C_{2v}</math></p>	 <p><math>a_2</math> <math>b_2</math> <math>\beta_1 = 1</math> <math>\beta_2 = .9</math> <math>E(a_2) = 0</math> <math>E(b_2) = 0</math></p>

Figure 1. Typical atomic orbital coefficients and energies of the "nonbonding" MO's for the different Hückel perimeters investigated.

adjacent carbon atoms and induces a reduction of length of the adjacent inner C-C bonds.

It is expected that the most detailed information regarding the structure of the radical anion will come from the esr spectrum, *viz.*, from the spin densities which can be approximated by the charge densities in the MO occupied by the unpaired electron. Since, in our elementary approach, it is not possible to know *a priori* which of the two Hückel nonbonding MO's is occupied by the unpaired electron (even if they are not degenerate in energy), we have established the analytical expressions giving the atomic orbital coefficients of the two nonbonding MO's<sup>21</sup> for each perimeter investigated. These expressions are given in the last column of Table I. Figure 1 gives, for the last four perimeters investigated, a schematic representation of the two nonbonding MO's<sup>21</sup> for the  $\beta$  values chosen; the symmetry of these orbitals and their energies are also given.

Several points are worth noting here: (1) For all the perimeters in which bond alternation is introduced (perimeters 2 and 3 in Table I) the two nonbonding HMO's are no longer degenerate. These orbitals have both different symmetry and different energy. (2) For all the perimeters in which bond alternation is not introduced (perimeters 1, 4, and 5 in Table I) the two nonbonding MO's are degenerate in energy but not necessarily in symmetry. (3) Bond alternation implies that symmetry elements such as  $C_2'$  axes or  $\sigma_v$  planes, if present, must pass through the mid-points of C-C bonds but not through C atoms. Since each of the two nonbonding MO's must have eight nodal points, bond alternation implies that these nodal

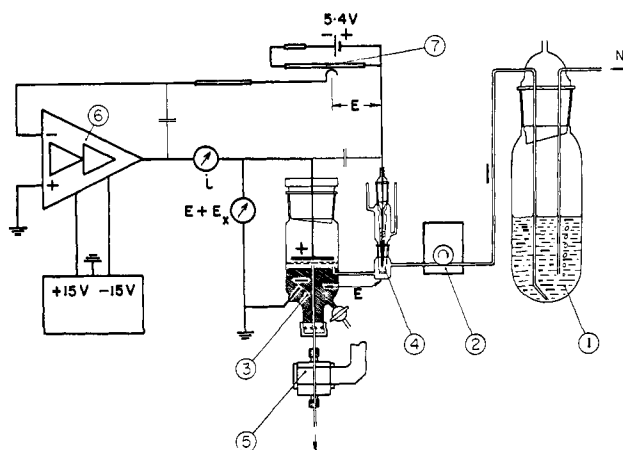


Figure 2. Apparatus for electrochemical reduction of a flowing solution under controlled potential: 1, stock solution; 2, pump; 3, Hg cathode; 4, reference electrode; 5, esr cavity; 6, potentiostat; the potential between the Hg cathode and the reference electrode is maintained at the value  $E$  selected on the potentiometer 7.

points can not all coincide with C atoms. In fact, for perimeters of  $D_{8h}$  symmetry (two  $\beta$  values; perimeter 2 in Table I) and of  $D_{4h}$  symmetry (three  $\beta$  values; perimeter 3) all atomic orbital coefficients are different from zero, independent of the  $\beta$  values chosen (*cf.* Figure 1). Thus, if eight atomic orbital coefficients in one nonbonding MO are found to be zero (for example, if eight protons of the radical anion are weakly coupled with the unpaired electron) then the chemical species investigated ( $R\cdot^-$ ) does not show bond alternation. Analogous arguments hold for any  $[4n]$ annulene.

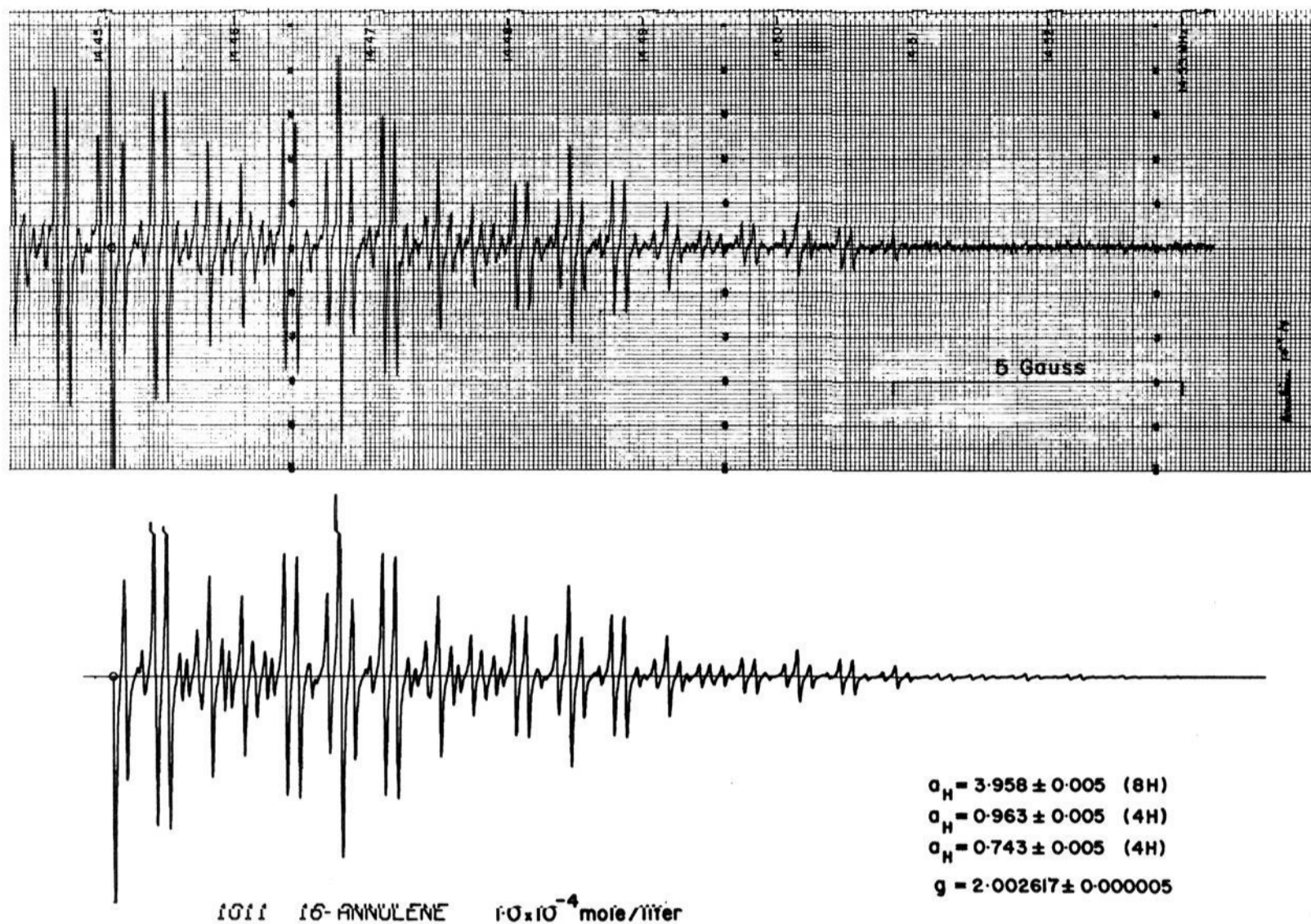


Figure 3. Experimental and simulated esr spectrum of the radical anion of [16]annulene.

## II. Experimental Section

**A. Polarography of [16]Annulene.** In our approach to the problem of preparing the radical anion and the dianion of [16]annulene, we first investigated the electrochemical reduction of [16]annulene by classical and by oscilloscopic polarography (one-shot triangular wave and continuous triangular wave).

In dimethylformamide (DMF), two reduction waves are observed and are found to be perfectly reversible (in the sweep frequency range of 0.05–250 Hz). They correspond to the processes indicated in Table II, *i.e.*, the reduction of [16]annulene to its radi-

**Table II.** Results from the Polarographic Study of the Reduction of [16]Annulene

	$E_{1/2}^a$	Reversibility	$ne^-$	Process
1st wave	-1.23	Reversible	$1e^-$	$R + 1e^- \rightleftharpoons R^{\cdot-}$
2nd wave	-1.52	Reversible	$1e^-$	$R^{\cdot-} + 1e^- \rightleftharpoons R^{2-}$

<sup>a</sup> The potentials  $E_{1/2}$  were measured at 0° with reference to the calomel electrode Hg|Hg<sub>2</sub>Cl<sub>2</sub>, aqueous 0.1 N KCl.

cal anion  $R^{\cdot-}$  and the reduction of the radical anion to the dianion  $R^{2-}$ .

**B. Electrochemical Preparation of the Radical Anion and of the Dianion of [16]Annulene.** Using the apparatus shown in Figure 2 in which the annulene solution (solvent, DMF; electrolyte, 0.05 M tetra-*n*-butylammonium perchlorate) is forced to flow continuously over the surface of the mercury cathode (the potential of which is maintained constant with respect to a calomel reference electrode), we could produce both species  $R^{\cdot-}$  (at -1.4 V) and  $R^{2-}$  (at -1.8 to 2.4 V). The flow rate  $dv/dt$  of the solution through the cell could be adjusted so that conditions for a 1:1 (for  $R^{\cdot-}$ ) or a 2:1 (for  $R^{2-}$ ) correspondence between the current  $i$  (expressed in Faradays (F) per second) and the flow rate (expressed in moles of annulene passing through the cell per second) could be obtained precisely.

**C. Electron Spin Resonance Spectrum of the Radical Anion  $R^{\cdot-}$**  By forcing the electrolyzed solution (at -1.4 V) through

a quartz capillary centered in the esr cavity, we could record the esr spectrum of the [16]annulene radical anion. Figure 3 shows a spectrum obtained under the following experimental conditions: solution, concentration, 10.3 mg of annulene in 500 ml of solvent (*i.e.*,  $1 \times 10^{-4}$  M); solvent, dimethylformamide; electrolyte, tetra-*n*-butylammonium perchlorate (0.05 M). Electrolysis conditions were: cathode potential, -1.3 V (reference, Hg|Hg<sub>2</sub>Cl<sub>2</sub>, aqueous KCl 0.1 N); current, 0.05 mA (*i.e.*,  $5.2 \times 10^{-10}$  F sec<sup>-1</sup>); flow rate,  $dv/dt = 4.5 \times 10^{-6}$  l. sec<sup>-1</sup>;  $dn/dt = 4.5 \times 10^{-10}$  mol sec<sup>-1</sup>.

The parameters deduced from the spectrum are listed in Table III. It can be seen that the experimental spectrum is exactly superimposable on that computed from these parameters.

**Table III.** Experimental ESR Parameters

8 equivalent H	$ a_H  = 3.958 \pm 0.005$ G
4 equivalent H	$ a_H  = 0.963 \pm 0.005$ G
4 equivalent H	$ a_H  = 0.743 \pm 0.005$ G
Line width	0.045 G

The  $g$  factor, obtained by comparison at the center of the spectrum of the microwave frequency and the <sup>1</sup>H-resonance frequency given by a field-tracking nmr gaussmeter, was found to be  $g = 2.002617 \pm 0.000005$ .

**D. Nmr Study of the Dianion  $R^{2-}$  of [16]Annulene.** We prepared the dianion for nmr spectroscopy studies by treating a solution of [16]annulene in THF-*d*<sub>8</sub> with an alkali metal. The potassium was distilled under high vacuum and contained 15 mg of annulene. THF-*d*<sub>8</sub> (0.3 ml) was then condensed on the annulene and the tube sealed off.

The nmr spectrum of the original solution was first recorded at -30° (one single line at  $\tau$  3.18). The solution was then brought into contact (at 0°) with the potassium by inverting the tube for a controlled time. The nmr and esr spectra were recorded (nmr at -30°) after each contact period. The nmr and esr observations are summarized in Figure 4. A very short contact time (less than 1 sec) produces a considerable broadening of the [16]annulene pro-

The reduction of [16]annulene into its dianion by potassium.

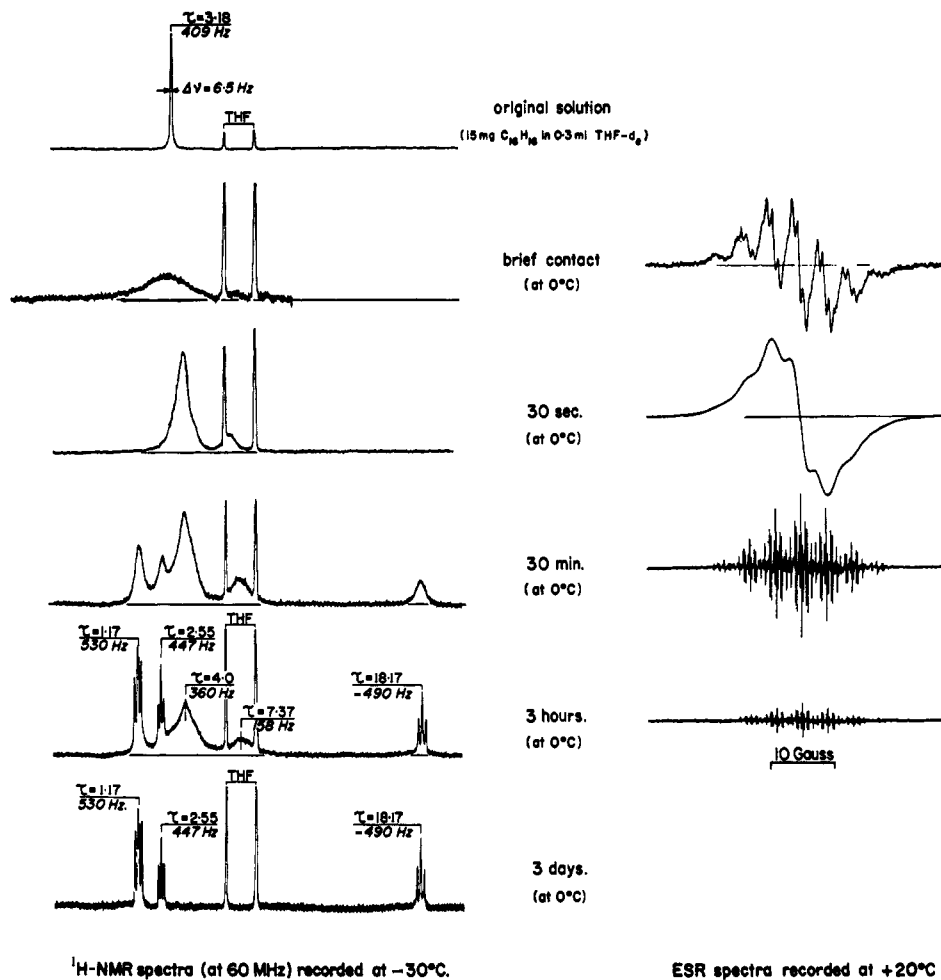


Figure 4. Nmr (60 MHz) and esr spectra of a [16]annulene solution for different contact times with potassium.

ton resonance line. This broadening is essentially due to the fast exchange  $R + R^{\cdot-} \rightleftharpoons R^{\cdot-} + R$  (the presence of an appreciable amount of radical anion  $R^{\cdot-}$  is indicated by a poorly resolved esr signal). After contact for 30 sec, two broad bands located at higher field ( $\tau$  4.0 and 7.3) than the initial [16]annulene line are observed in the nmr spectrum; at this stage the most intense but unresolved esr signal is observed. As the contact time of the solution with potassium is increased, these bands progressively disappear, while three new well-resolved signals develop. These new signals located at  $\tau$  1.17, 2.55, and 18.17 (relative intensities 8:4:4) are the only ones observable after 3 days contact and they remain unchanged if the contact is prolonged for several weeks. This indicates that the reduction of the [16]annulene to its dianion is complete (only a very weak esr signal is observed). We thus assign this final spectrum to the pure dianion, more specifically to the dianion of [16]-85-annulene.

The origin of the two nmr bands at  $\tau$  4.0 and 7.37 (see spectra after 30-sec, 30-min, and 3-hr contact time in Figure 4) is not yet clear. We do not think that these signals can be attributed either to the neutral molecule or to the dianion, since they appear simultaneously with the signal of the former in spectra recorded for short contact times (10 and 20 sec; not shown in Figure 4) and they appear simultaneously with the signals of  $R^{2-}$  in the nmr spectra recorded for contact times longer than 10 min (e.g., after 30 min and 3 hr; see Figure 4). On the other hand, it seems unlikely that the bands in question could be due to the paramagnetic species  $R^{\cdot-}$  in view of the magnitude of the hyperfine splittings observed in the esr spectrum. Further experimental work is required (esr and nmr spectra at variable temperature after short contact times with the alkali metal) in order to elucidate the origin of these bands.

The same experiment was carried out with sodium and with lithium. (All metals were extruded *in vacuo* directly into the nmr tube.) The same modifications of the esr and nmr spectra were observed, with the difference that the reaction with lithium was much slower than with potassium or sodium; the final spectrum of the pure dianion lithium salt could be observed only after 6 days. The positions of the three signals are not affected significantly by the nature of the cation, as can be seen from Table IV.

The comparison of the spectra of [16]annulene (recorded at  $-140^\circ$ ) and of its dianion (as the lithium salt) is illustrated in Figure 5. In Table IV we summarize the nmr parameters deduced for both species ([16]-85-annulene and [16]-85-annulene dianion) and for [18]annulene.

**E. Visible and Uv Spectra of [16]Annulene and of Its Radical Anion  $R^{\cdot-}$  and Dianion  $R^{2-}$ .** By circulating the electrolyzed solution through an optical cell adapted to a Cary-14 spectrophotometer we could record the visible and uv spectra of both  $R^{\cdot-}$  and  $R^{2-}$ .

Typical spectra were obtained under the following experimental conditions: solution, concentration, 20.4 mg of annulene in 280 ml of solvent (i.e.,  $3.50 \times 10^{-4} M$ ); solvent dimethylformamide; electrolyte tetra-*n*-butylammonium perchlorate (0.05 *M*). The optical cell had  $e = 0.0370$ -cm optical path. Electrolysis conditions for producing the radical anion  $R^{\cdot-}$  and the dianion  $R^{2-}$ , respectively, were: cathode potential,  $R^{\cdot-}$ ,  $-1.4$  V (reference  $Hg|Hg_2Cl_2$ , aqueous KCl 0.1 *N*);  $R^{2-}$ ,  $-2.0$  V; current,  $R^{\cdot-}$ , 0.085 mA (i.e.,  $8.8 \times 10^{-10}$  F sec $^{-1}$ );  $R^{2-}$ , 0.18 mA (i.e.,  $18.65 \times 10^{-10}$  F sec $^{-1}$ ); flow rate,  $dv/dt = 2.5 \times 10^{-6}$  l. sec $^{-1}$ ; i.e.,  $dn/dt = 8.75 \times 10^{-10}$  mol sec $^{-1}$ . These spectra are reproduced, together with the spectrum of [16]annulene, in Figure 6. The absorption maxima and the corresponding extinction coefficients are listed in Table V.

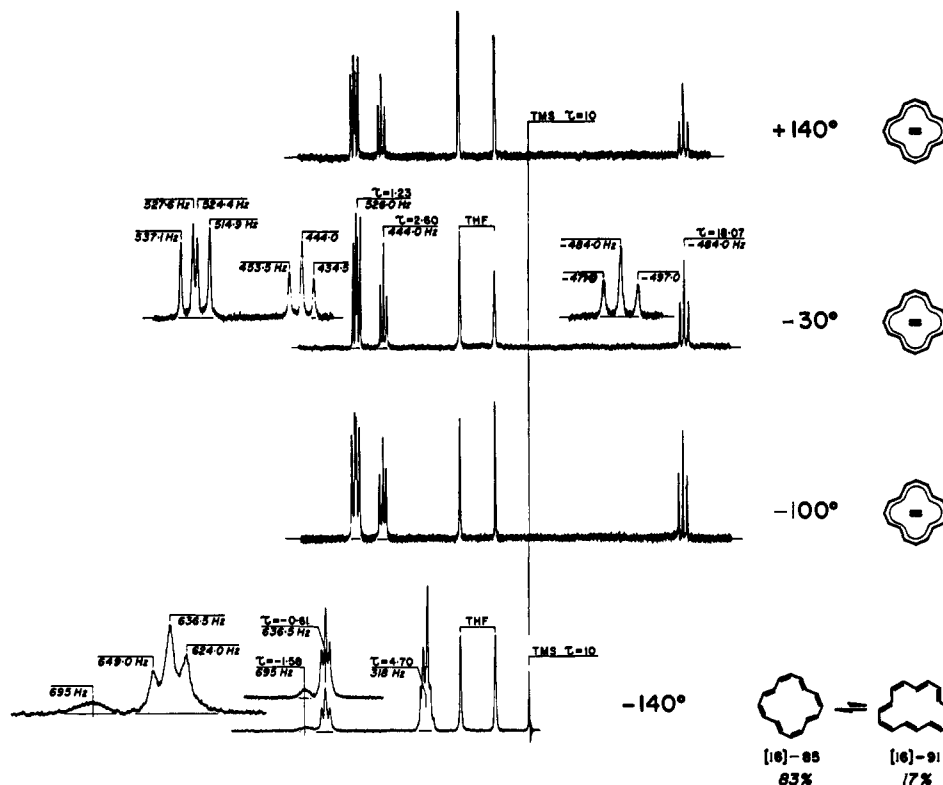


Figure 5. Nmr (60 MHz) spectrum of [16]annulene dianion recorded at three different temperatures. The spectrum of [16]annulene at  $-140^\circ$  is reproduced on the same scale for comparison.

F. **Stability of the Radical Anion  $R\cdot^-$ .** If the potential of the mercury cathode is maintained at  $-2.0$  V (or at a more negative value) and the flow rate of the solution is adjusted so that 1 F is

transferred per mole of [16]annulene, the uv-visible spectrum indicates that the main species in the electrolyzed solution is the radical anion  $R\cdot^-$ . Under the same conditions, the esr spectrum of the

Table IV. Nmr Parameters for [16]-85-Annulene, [16]-85-Annulene Dianion, and [18]Annulene

Species			
Aromatic character	Nonaromatic	Aromatic	Aromatic
Geometry	Nonplanar	Most likely planar	Planar
Symmetry	$S_4$	$D_{4h}$	$D_{6h}$
Total no. of different chemical shifts	4	3	2
$\tau$ values	$-120^\circ$ $\tau_A = -0.53$ $\tau_B = \tau_D = +4.60$ $\tau_C = +4.89$	$-30^\circ$ Li <sup>+</sup> Na <sup>+</sup> K <sup>+</sup> $\tau_A$ 18.07 18.03 18.17 $\tau_B$ 1.23 1.05 1.17 $\tau_C$ 2.60 2.45 2.55	$-60^\circ$ $\tau_A = 12.88$ $\tau_B = 0.75$
$J$ values <sup>a</sup>	$-120^\circ$ $(J_{AB} + J_{AD})/2 = 12.5$ $(J_{BC} + J_{CD})/2 = 9.0$ $J_{AC} = 0, J_{BD} = -1$	$-30^\circ$ $J_{AB}$ 13.0 13.2 12.7 $J_{BC}$ 9.5 9.5 9.8	$-60^\circ$ $J_{AB} = 13.5$ $J_{AB'} = -1.05$ $J_{BB'} = 8.0$
Calcd contributions due to ring current, <sup>b</sup> $\Delta\tau^{RC}$		$\Delta\tau_A^{RC} = 16.3$ $\Delta\tau_B^{RC} = -5.8$ $\Delta\tau_C^{RC} = -4.8$	$\Delta\tau_A^{RC} = 18.4$ $\Delta\tau_B^{RC} = -5.8$
Calcd contributions due to negative charges, $\Delta\tau^{2-}$		$\Delta\tau_A^{2-} = 0.4$ $\Delta\tau_B^{2-} = 1.4$ $\Delta\tau_C^{2-} = 0.4$	
Calcd chemical shifts, $\tau_{calcd}$		$\tau_A = 20.9$ $\tau_B = -0.2$ $\tau_C = -0.2$	$\tau_A = 22.6$ $\tau_B = -1.6$

<sup>a</sup> In hertz. <sup>b</sup> The ring current is calculated for the regular polygons according to the method of F. London, *J. Phys. Radium*, **8**, 397 (1937). However, the real geometry has been used for calculating the geometrical factors in the expression  $\Delta\tau^{RC}$ .

Table V. Absorption Maxima and Extinction Coefficients (Visible and Uv) of [16]Annulene and of Its Radical Anion R<sup>•-</sup> and of Its Dianion R<sup>2-</sup> -

Chem species	Correl no. of transit	$\lambda_{\text{max}}$ , nm	Exptl data $\bar{\nu}$ , cm <sup>-1</sup>	$\epsilon$	Assignments of the transitions assuming $D_{16h}$ perimeter Symmetry			Assignments of the transitions assuming the point group indicated Symmetry			
					Transitions between MO's	Transitions between states	Selection rule <sup>a</sup>	Point group	Transitions between MO's	Transitions between states	Selection rule <sup>a</sup>
R	1	446	22,410	588	$e_{1u} \rightarrow e_{1u}$	$A_{1g} \rightarrow A_{1g}$	$f$	$S_4$	$2b \rightarrow 3b$	$A \rightarrow A$	$f$
	3	293	34,120	78,500	$e_{1u} \rightarrow e_{1g}$	$A_{1g} \rightarrow E_{1u}$	$a$		$2b \rightarrow 3e$	$A \rightarrow E$	$a$
	1		Not obsd		$e_{1u} \rightarrow e_{1u}$	$E_{1u} \rightarrow E_{1u}$	$f$	$D_{4h}$	$2a_{2u} \rightarrow a_{1u}$	$A_{1u} \rightarrow A_{2u}$	$f$
R <sup>•-</sup>	2	{664 690}	{15,050 14,490}	{10,600 10,000}	$e_{1u} \rightarrow e_{1g}$	$E_{1u} \rightarrow E_{1g} + 2E_{3g}$	$f$		$a_{1u} \rightarrow 3e_g$	$A_{1u} \rightarrow E_g$	$a$
	3	380	26,300	190,000	$e_{1u} \rightarrow e_{1g}$		$a$		$2a_{2u} \rightarrow 3e_g$	$A_{1u} \rightarrow E_g$	$a$
	4	330	30,020	51,500	$e_{1g} \rightarrow e_{1u}$	$E_{1u} \rightarrow E_{3g}$	$a$		$2e_g \rightarrow a_{1u}$	$A_{1u} \rightarrow E_g$	$a$
	2	{560 600}	{17,850 16,600}	{13,750 15,800}	$e_{1u} \rightarrow e_{1g}$	$A_{1g} \rightarrow E_{1u}$	$f$	$D_{4h}$	$a_{1u} \rightarrow 3e_g$	$A_{1g} \rightarrow E_u$	$a$
R <sup>2-</sup>	3	412	24,260	175,000	$e_{1u} \rightarrow e_{1g}$	$A_{1g} \rightarrow E_{1u}$	$a$		$2a_{2u} \rightarrow 3e_g$	$A_{1g} \rightarrow E_u$	$a$

<sup>a</sup>a = allowed; f = forbidden.

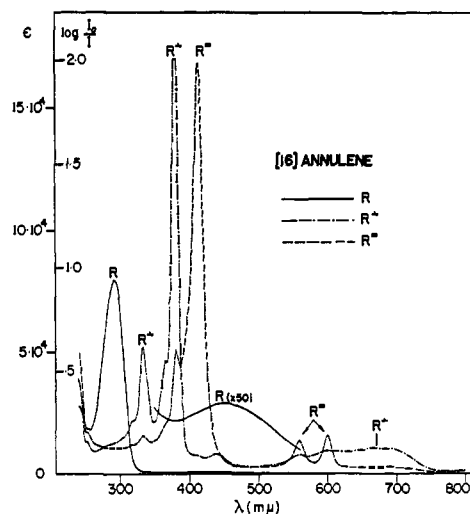


Figure 6. Absorption spectra (visible and uv) of [16]annulene, [16]annulene radical anion, and [16]annulene dianion.

radical anion is observed at its maximum intensity. It is thus clear that the dianion (which is certainly formed at the cathode) reacts immediately with R to produce  $2R^{\bullet-}$  as soon as it diffuses away from the cathode. In other words, the disproportionation equilibrium



is strongly in favor of the radical anion.

Under aprotic conditions, the radical anion of [16]annulene is a quite stable species. Even at 90° its half-life is very long (at least several hours), as judged by the observation that the intensity of the esr spectrum decays only very slowly when the flow of the electrolyzed solution is stopped.

**G. Dynamic Behavior and Thermal Stability of the [16]Annulene Dianion.** In order to investigate any dynamic behavior of the dianion that could possibly be detected by nmr spectroscopy, we have recorded its spectrum at different temperatures ranging from -100 to +140°. We have carried out these measurements, on the lithium salt of the dianion, since this was found to be the most soluble salt at low temperatures. Some spectra are reproduced in Figure 5.

Apart from very small displacements of their position, neither broadening nor any minor modification of the fine structure of the resonance signals was observed, as can be seen in Figure 5. This means that such a dynamic behavior as observed in the case of [18]annulene,<sup>7</sup> by which all the protons become equivalent in the nmr spectrum, does not take place here.

Finally, it should be mentioned that the thermal stability of the dianion of [16]annulene is very great. Heating the nmr tube for 8 days at 100° has no influence whatsoever; the nmr spectra recorded under identical conditions before and after heating do not show any new signals, nor any decay in intensity.

### III. Discussion

**A. Structure of the Radical Anion. The ESR Spectrum.** The esr spectrum of the radical anion of [16]annulene indicates that the unpaired electron is strongly coupled with a set of eight equivalent protons ( $|a_H| = 3.958$  G) and weakly coupled with two sets of four equivalent protons ( $|a_H| = 0.963$  and 0.743 G). The small splittings are likely to correspond to negative spin densities. If we assume that the relation of McConnell<sup>22</sup> is a good approximation, then the width of

$$a_H = Q\rho$$

the esr spectrum is a measure of  $|Q|$  if all spin densities are positive. This width is 38.5 G, a value which is much larger than normal values of  $|Q|$  for the radical

(22) H. M. McConnell, *J. Chem. Phys.*, 24, 632, 764 (1956).



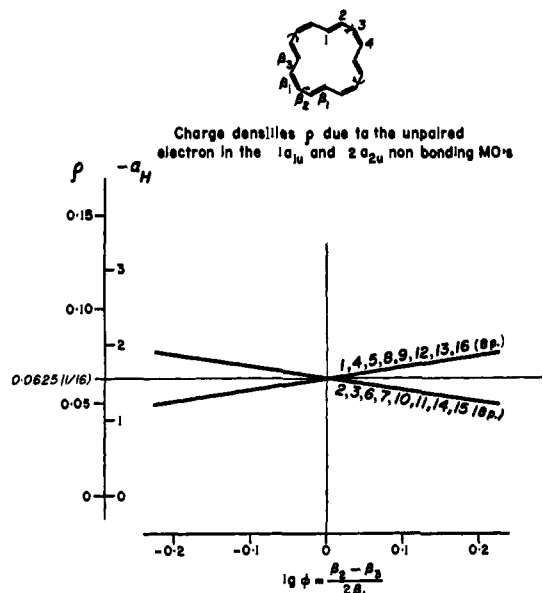


Figure 7. Perimeter of type 3 (geometry of the neutral molecule, *i.e.*,  $S_4$  symmetry): charge densities  $\rho$  in the two "nonbonding" MO's and hyperfine splittings  $a_H$  expected as functions of the values of  $\beta_1$  and  $\beta_2 - \beta_1$ , the unpaired electrons being in the  $1a_{1u}$  and  $2a_{2u}$  nonbonding MO's.

anions of conjugated hydrocarbons.<sup>13,23</sup> On the contrary, if one assumes that the two smaller spin densities are negative, one finds  $|Q| = 24.84$  G, a value which compares favorably with the value  $|Q| = 25.7$  G found for the radical anion of cyclooctatetraene.<sup>24</sup> This leaves little doubt that the sign of the smaller coupling constants is opposite to that of the larger one. The corresponding charge densities in the MO occupied by the unpaired electron must then be negative (in the Hückel approximation, they must then be zero<sup>25</sup>). Consequently, according to what was said above (*cf.* section I-B) the radical anion *does not exhibit bond alternation, but has a delocalized 17-electron  $\pi$ -bond system.*

The second and third perimeters investigated (*cf.* Table I) are consequently incompatible with the observed esr spectrum. Indeed, in the case of the second one the charge densities  $\rho$  due to the unpaired electron are all equal (independently of the  $\beta$  values chosen), implying *one* identical coupling of the electron with each of the 16 protons; in the case of the third perimeter (a corresponding geometry is that of the neutral [16]-85-annulene) one expects the unpaired electron to be strongly coupled with two sets of eight equivalent protons, independently of the nonbonding MO which it occupies<sup>26</sup> and of the  $\beta$  values chosen; this is illustrated by Figure 7.

The last two perimeters investigated (perimeters 4 and 5 in Table I) corresponding to delocalized  $\pi$  systems are thus the relevant ones to be discussed. They correspond to the planar delocalized structures derived from the 85 and 91 configurations, respectively. The charge densities due to the unpaired electron are given

(23) H. M. McConnell, *J. Chem. Phys.*, **28**, 107 (1958).

(24) A. Carrington and P. F. Todd, *Mol. Phys.*, **7**, 533 (1963).

(25) A. D. McLachlan, *ibid.*, **3**, 233 (1970).

(26) The two nonbonding MO's are not degenerate in symmetry, but are degenerate in energy. Their symmetries are  $a_{1u}$  and  $a_{2u}$  in the  $D_{4h}$  and b in the  $S_4$  point groups.

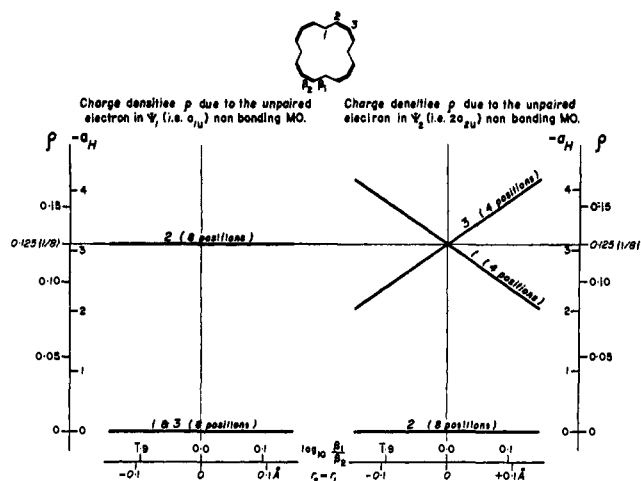


Figure 8. Perimeter of type 4 ( $D_{4h}$  symmetry); charge densities  $\rho$  and hyperfine splittings  $a_H$  expected as function of the values of  $\beta_1/\beta_2$ , the unpaired electron being in the  $a_{1u}$  (left) or in the  $2a_{2u}$  (right) MO.

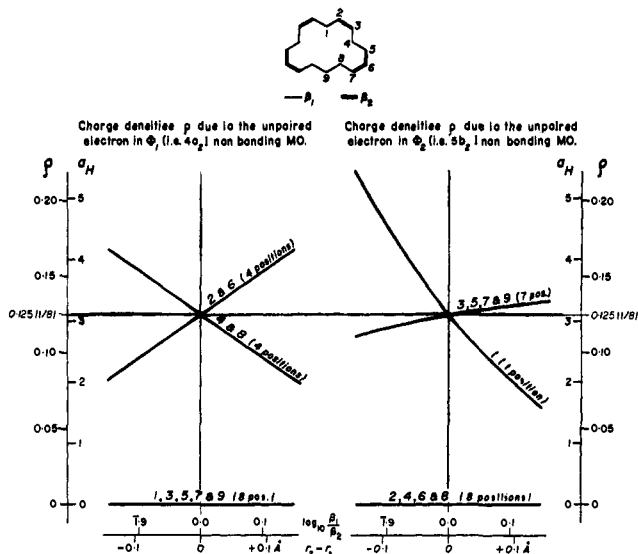


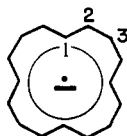
Figure 9. Perimeter of type 5 ( $C_{2v}$  symmetry); charge densities  $\rho$  and hyperfine splittings  $a_H$  expected as function of the value of  $\beta_1/\beta_2$ , the unpaired electron being in the  $4a_2$  (left) or in the  $5b_2$  (right) MO. ( $a_H$  should read  $-a_H$ .)

in Figures 8 and 9,<sup>21</sup> as a function of the resonance integrals  $\beta_1$  and  $\beta_2$  (*i.e.*, of  $\log(\beta_1/\beta_2)$ ) introduced to impose the symmetries  $D_{4h}$  and  $C_{2v}$ . In order to exhibit the order of magnitude of the effects involved, the variation of the resonance integrals in Figures 8 and 9 have also been expressed in terms of bond-length variation. For this we have used the relationship  $\beta = -38.47 \exp[(1.397 - r)/0.4096]$  kcal mol<sup>-1</sup>, which is derived by the method of Longuet-Higgins and Salem<sup>14</sup> from the best benzene force constants found by Duinker.<sup>27</sup> The figures show that the qualitative features of the density pattern vary significantly with minor modifications of the structure and from one orbital to the other in the pairs.

The only relevant orbital with a charge distribution in accordance with that deduced from the esr spectrum (eight positions with equal and high charge density,

(27) J. C. Duinker, Ph.D. Thesis, University of Amsterdam, 1964.

eight positions with zero charge density) is the  $a_{1u}$  MO of the delocalized structure of the 85 configuration (fourth perimeter in Table I and Figure 8, left side). The  $D_{4h}$  point group symmetry of this structure agrees also with the existence of *two* small coupling constants of the electron with *two* sets of four protons. These two sets are the four inner and the four outermost protons, respectively. Hückel calculations cannot predict that two different splitting constants will correspond to these two sites, and, *a fortiori*, their attribution cannot be made. As a conclusion, we attribute the observed esr spectrum to the delocalized 85 configura-



[16]-85-annulene radical anion

tion with the following signs and assignments for the hyperfine splittings (Table VI).

**Table VI.** Assignments of the Hyperfine Splittings Occurring in the ESR Spectrum of the Radical Anion of [16]Annulene

$a_H = -3.958$ G	8 equivalent H on position 2
$a_H = +0.963$ G	4 equivalent H on positions 1 or 3
$a_H = +0.743$ G	4 equivalent H on positions 3 or 1

In order to further substantiate our interpretation, we have calculated the charge densities according to McLachlan's formula<sup>28</sup>

$$a_{H_i} = Q(\rho_i^{\text{Hückel}} + \Delta\rho_i)$$

with

$$\Delta\rho_i = k \sum_j^n \pi_{ij} \rho_j^{\text{Hückel}}$$

$$k = 1.2 \text{ (semiempirical value)}$$

but simply using for the atom-atom polarizabilities  $\pi_{ij}$  the values obtained in our simple HMO computations. The results of these calculations are summarized in Figure 10; they show that zero charge densities in the Hückel approximation indeed correspond to negative charge densities and that two sets of four weakly coupled protons must be expected.

The  $g$  value of the radical anion is in good agreement with that predicted for a radical anion with the unpaired electron in a nonbonding MO. According to Stone's semiempirical formula<sup>29</sup>

$$\Delta g = g - g_0 = b - \lambda c$$

where  $g$  is the  $g$  factor corrected for the second-order shifts,  $g_0$  is the  $g$  factor for a free electron ( $g_0 = 2.00231924$ ),  $\lambda$  is the coefficient of  $\beta$  in the expression of the energy of the Hückel MO occupied by the unpaired electron, and  $b$  and  $c$  are empirical coefficients. All radicals with the unpaired electron in a nonbonding MO ( $\lambda = 0$ ) should have the same  $g$  factor, namely:  $g = 2.0026382$  ( $b = 31.9 \times 10^{-5}$ <sup>30</sup>). Our value,

(28) A. D. McLachlan, *Mol. Phys.*, **3**, 233 (1960).

(29) A. J. Stone, *ibid.*, **6**, 509 (1963).

(30) B. G. Segal, M. Kaplan, and G. K. Fraenkel, *J. Chem. Phys.*, **43**, 4191 (1965).

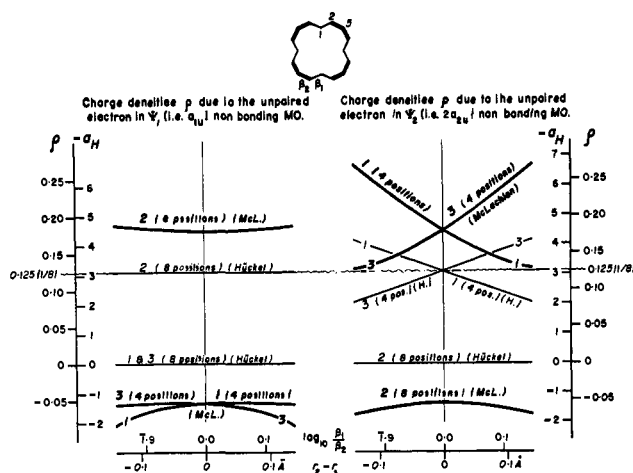
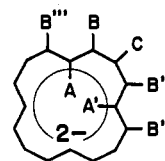


Figure 10. Perimeter of type 4 ( $D_{4h}$  symmetry); charge densities  $\rho$  and hyperfine splittings  $a_H$ , according to McLachlan, expected as function of the value of  $\beta_1/\beta_2$ , the unpaired electron being in the  $a_{1u}$  (left) or in the  $2a_{2u}$  (right) MO.

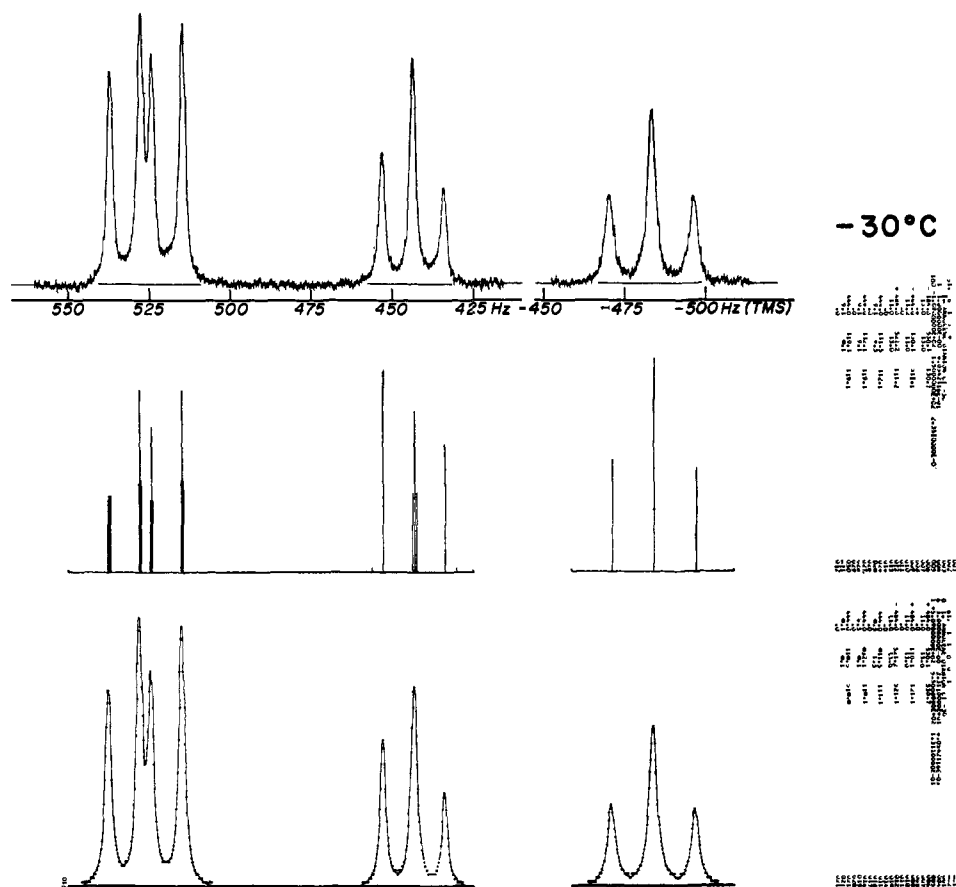
corrected for the second-order shifts  $g = 2.002617 - 6.0 \times 10^{-6} = 2.002611 \pm 0.000005$ , does not differ by more than  $2 \times 10^{-5}$  from this theoretical value.

**The UV-Visible Absorption Spectrum.** The absorption spectrum of the radical anion (Figure 6) supports the conclusions drawn from the esr spectrum. The two absorption bands at 330 and 380 nm are extremely sharp while the band at 660–690 nm shows some vibrational structures. This clearly indicates that the radical anion must have a high symmetry and no bond alternation. We will see later that the number of transitions observed and their symmetry can be correctly predicted with our elementary approach. However, the quantitative use of the intensities and of the frequencies of the transitions for structural identification would require more elaborate semiempirical MO calculations (Pariser, Parr, and Pople).

**B. Structure of the Dianion. The Nmr Spectrum.** Since the radical anion has a structure derived from the 85 configuration with  $D_{4h}$  symmetry, it is to be expected that the dianion will have an analogous structure and will also show  $\pi$ -bond delocalization. This is confirmed by the quantitative analysis of the nmr spectrum of the lithium salt of the dianion (Figure 5). Three signals of relative intensities 8:4:4 and chemical shifts  $\tau$  1.23, 2.60, and 18.07, respectively, are observed. The simple triplet structure of the signal at  $\tau$  18.07 shows immediately that the dianion has four isochronous internal protons A, A', A'', A''', and that each proton A is equally coupled with two protons (B and B'') with a coupling constant of 13.0 Hz. The B protons are ob-



viously responsible for the absorption at  $\tau$  1.23. Since their signal is a doublet of doublets, one deduces that: (1) each proton B is coupled to the vicinal protons of type A and C with coupling constants  $J_{AB} = J_{AB''} = 13.0$  and  $J_{BC} = J_{B'C} = 9.5$  Hz; (2) all protons B are isochronous. The simple triplet structure of the signal



**[16]annulene dianion (as lithium salt)**

Figure 11. Comparison of the observed and computed  $^1\text{H}$  nmr signals of the outer (left) and inner (right) protons of the [16]annulene dianion.

for the C protons (at  $\tau$  2.60) indicates that these protons are also isochronous.

From the point of view of nmr spectroscopy, it follows that the dianion of [16]annulene has the 85 configuration and exhibits  $\pi$ -bond delocalization. Its symmetry is most likely  $D_{4h}$  ( $D_4$  and  $D_{2d}$  are also possible symmetries since only the following symmetry elements must be present: a  $C_4$  or a  $S_4$  axis, two  $C_2'$  axes or two  $\sigma'$  planes). One must of course consider the possibility that the isochronism of the eight B protons and the identity of the coupling  $J_{AB}$  and  $J_{AB''}$  (and therefore the implied symmetry) are the result of a very fast valence bond isomerization. This is ruled out on the basis of the optical spectrum of  $\text{R}^{2-}$  which is composed of extremely sharp bands, one exhibiting a clearly resolved vibrational structure. Were the dianion a localized  $\pi$ -bond system (but exhibiting an extremely fast  $\pi$ -bond shift), the electronic spectrum would consist of much broader bands, as is the case for the neutral [16]annulene molecule itself.

A fitting of the computed to the experimental nmr spectrum was also made and is shown in Figure 11. The signal of the external protons has been computed assuming that one can neglect the coupling constants of the B and C protons with all the other protons except A and A'. In view of the large difference in chemical shifts between B and C on the one hand, and A on

the other, we have used the method of effective chemical shifts for taking into account the coupling with A and A'.<sup>31</sup> In the same way, the signal of the internal protons has been considered to be the A part of a BAB''' system in which the coupling between B and C, and B''' and C, is also taken into account by the method of effective chemical shifts. The parameters giving the best fit are listed in Table IV; they can be compared to corresponding parameters observed with [16]- and [18]annulene.

The diamagnetism associated with the delocalized 18 electrons in the [16]annulene dianion is clearly demonstrated by the fact that the resonance signal of the inner protons appears at extremely high field ( $\tau$  18.17) (diamagnetic ring current), while the signals due to the outer protons appear at lower field [ $\tau$  1.17 (8 H) and 2.55 (4 H)] than those of normal olefinic protons, despite the shielding effect due to the extra negative charges. Thus, going from a  $4n$   $\pi$ -electron system ([16]-85-annulene) to a  $(4n + 2)$   $\pi$ -electron system (dianion of [16]-85-annulene) results in the inner proton resonance signal moving from very low field ( $\tau$  -0.50) (paramagnetic ring current)<sup>32</sup> to very high field ( $\tau$

(31) S. Diehl, R. G. Jones, and H. J. Bernstein, *Can. J. Chem.*, **43**, 81 (1965).

(32) J. A. Pople and K. G. Untch, *J. Amer. Chem. Soc.*, **88**, 4811 (1966).

**Table VII.** Kinetic Parameters and Delocalization (DE) and Resonance (RE) Energies for the [16]Annulene Dianion (Hypothetical Conformational Mobility), [18]Annulene (Conformational Mobility), and [16]-85- and [16]-91-Annulene ( $\pi$ -Bond Shift)

Parameters	Units	[16]Annulene <sup>2-</sup>	[18]Annulene	[16]-85-Annulene	[16]-91-Annulene
$p$ (0°) <sup>a</sup>	sec <sup>-1</sup>		18.2	$625 \times 10^3$	$17 \times 10^6$
$p$ (140°)	sec <sup>-1</sup>	<5	$0.4 \times 10^6$	$200 \times 10^6$	$3 \times 10^9$
$\Delta G^\ddagger$ (140°)	kcal mol <sup>-1</sup>	>25	13.5	8.9	6.6
$\Delta H^\ddagger$ (140°)	kcal mol <sup>-1</sup>	>28 <sup>d</sup>	16.1	8.2	7.7
DE (HMO) <sup>b</sup>	$\beta$ units <sup>c</sup>	-6.11	-5.04	-4.11	-4.11
	kcal mol <sup>-1</sup>	92.9	76.5	62.5	62.5
RE (PPP) <sup>b</sup>	kcal mol <sup>-1</sup>		8.81		0.99
RE (SPO)	kcal mol <sup>-1</sup>		6.39		-3.11

<sup>a</sup> References 34 and 35. <sup>b</sup> Reference 37. <sup>c</sup>  $\beta = -15$  to  $-18$  kcal<sup>13</sup> ( $-15.2$  adopted). <sup>d</sup> Assuming the same  $\Delta S^\ddagger$  value as for [18]annulene, *i.e.*,  $\Delta S^\ddagger = 6.4$  cal mol<sup>-1</sup> deg<sup>-1</sup>.

18.17) (diamagnetic ring current),<sup>32</sup> while the outer proton signals move from  $\tau$  4.70 to 1.17 and 2.55 (*cf.* Figure 5). The magnitude of the diamagnetic shift shows also that the dianion must be planar. We have estimated diamagnetic shifts  $\Delta\tau^{\text{RC}}$  due to the ring current in the dianion of [16]annulene and in the isoelectronic [18]annulene. The ring current  $J$  was first computed according to the theory of London<sup>33</sup> for a Hückel perimeter. The following relation was used

$$J = \frac{16\pi^2\beta e^2 S}{h^2 n^2 C} H \Sigma$$

where  $S$  is the surface of the ring,  $H$  is the applied magnetic field,  $\beta$  is the Bohr magneton, and  $e$ ,  $h$ , and  $c$  have their usual meanings, but  $n = 16$ ,  $\Sigma = \cot(\pi/16)$  for the dianion of [16]annulene, and  $n = 18$ ,  $\Sigma = \csc(\pi/18)$  for [18]annulene. The diamagnetic shifts  $\Delta\tau^{\text{RC}}$  have then been computed by summing up the contribution of each segment of the *true* molecular perimeter. The geometry of the dianion of [16]annulene has been determined in the following way: the same bond lengths as in [18]annulene (*i.e.*, 1.38 Å for inner bonds and 1.42 for the outer bonds) have been chosen and the bond angles have been calculated by minimizing the strain energy, taking 125° as the equilibrium unstrained C-C-C bond angle. The results of these calculations ( $\Delta\tau^{\text{RC}}$ ) are given in Table IV. The contributions to the chemical shifts  $\Delta\tau^{2-}$  due to the extra negative charges in the dianion have also been calculated from estimated charge densities; they are much less important than the ring current contributions but nevertheless are significant (see Table IV). Finally, the  $\tau$  values were calculated taking the value  $\tau_{\text{olef}} 4.2$  for the chemical shift of normal olefinic protons. As can be seen from Table IV, the calculated shifts are in relatively good agreement with the experimental one in the case of the dianion of [16]annulene, but not in the case of [18]annulene (unless we extrapolate the [18]annulene shifts to absolute zero temperature<sup>34</sup>).

**C. The Absence of Conformational Mobility and the Thermal Stability of the [16]Annulene Dianion.** A dynamic process by which the inner and outer protons would exchange their magnetic sites does not take place in the dianion of [16]annulene; the spectra recorded at  $-100$  and  $+140^\circ$  are identical (Figure 5). This is in complete contrast with the dynamic behavior of [16]-<sup>3</sup> and [18]annulene.<sup>7,34</sup> If one accepts the idea that the

enthalpy of activation of the conformational mobility in the aromatic annulenes of large size ([14]-, [18]annulene) represents essentially the energy required to overcome the resonance energy associated with the delocalized  $(4n + 2)$   $\pi$ -electron system,<sup>34,35</sup> then one has to conclude that the resonance energy in the [16]-annulene dianion is greater than in the isoelectronic [18]annulene. The activation enthalpy for the conformational mobility in [18]annulene was found to be  $\Delta H^\ddagger = 16.1$  kcal mol<sup>-1</sup> ( $\Delta G^\ddagger(140^\circ) = 13.46$  kcal mol<sup>-1</sup>); from this experimental value it is possible to deduce, using thermochemical arguments, that the resonance energy associated with the delocalized 18-electron  $\pi$ -bond system must be smaller than 19 kcal mol<sup>-1</sup>.<sup>34</sup> The fact that the dianion of [16]annulene does not show any sign of nmr exchange at 140° implies that the activation free-energy  $\Delta G^\ddagger(140^\circ)$  of a possible exchange process is certainly greater than 25 kcal mol<sup>-1</sup> (*i.e.*, *ca.* 12 kcal mol<sup>-1</sup> greater than in [18]annulene). This would indicate that the resonance energy of the [16]annulene dianion is at least 12 kcal mol<sup>-1</sup> greater than the resonance energy of [18]annulene, its isoelectronic neutral analog. Simple HMO calculations<sup>36</sup> confirm this conclusion and indicate that the delocalization energy<sup>13,37</sup> in the [16]annulene dianion is 16–19 kcal mol<sup>-1</sup> ( $-1.07$   $\beta$  unit;  $\beta = -15$  to  $-18$  kcal)<sup>13</sup> greater than in [18]annulene. We should point out here that simple HMO calculations predict that the delocalization energy (and thus the resonance energy) in the annulenes should increase with ring size (in the  $[4n + 2]$  and the  $[4n]$ annulenes). This is in contradiction with the conclusion that we have drawn from the quantitative study of the dynamic behavior of the annulenes;<sup>35</sup> the resonance energy was found to be very small ([16]annulene) or even negative (COT, *i.e.*, [8]annulene) in the case of the  $[4n]$ annulenes, and positive but decreasing with ring size ([14]- and [18]annulene) in the case of the  $[4n + 2]$ annulenes. These conclusions are supported by the semiempirical MO calculations (Pariser, Parr, Pople, and split p orbitals) of Dewar and Gleicher.<sup>37</sup> Table VII shows the parallelism which exists between the computed delocalization energy DE (simple HMO calculations<sup>36</sup>) or the computed resonance energy RE (semiempirical MO calculations<sup>37</sup>) and the enthalpy of activation  $\Delta H^\ddagger$  for the dynamic process responsible for the exchange of internal and external protons in the *aromatic planar*<sup>11,12</sup>

(35) J. F. M. Oth, *Pure Appl. Chem.*, **24**, 573 (1971).

(36) J. F. M. Oth and J.-M. Gilles, unpublished results.

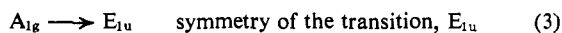
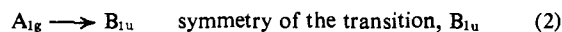
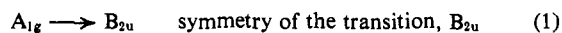
(37) The delocalization energy (DE) and the resonance energy (RE) here have the same significance as discussed by M. J. S. Dewar and G. J. Gleicher, *J. Amer. Chem. Soc.*, **87**, 685 (1965).

(33) See London, Table IV, footnote *b*.

(34) J.-M. Gilles, J. F. M. Oth, F. Sondheimer, and E. P. Woo, *J. Chem. Soc. B*, 2177 (1971).



transitions (considering the  $D_{nh}$  symmetry of the simple Hückel perimeter)



and their positions  $\bar{\nu}$  are predicted and found to be a linear function of  $\sin \pi/n$ . The  $A_{1g} \rightarrow E_{1u}$  transition in [16]annulene dianion has to be correlated with the transition  $A_{1g} \rightarrow E_{1u}$  of the aromatic annulenes and is expected to appear at about 28,000  $\text{cm}^{-1}$  (observed at 24,260  $\text{cm}^{-1}$ ); the degenerate transition  $A_{1g} \rightarrow E_{7u}$  has to be correlated with the two nondegenerate transitions  $A_{1g} \rightarrow B_{1u}$  and  $A_{1g} \rightarrow B_{2u}$  of the aromatic annulenes and is expected to appear at about 19,500  $\text{cm}^{-1}$  (observed at 17,250  $\text{cm}^{-1}$ ). Figure 13 shows how the above-mentioned correlation between the three transitions in the aromatic annulene and the two transitions observed in the dianion of [16]annulene was established. Note that the two broad transitions observed in the dianion of cyclooctatetraene<sup>41</sup> are also found at their predicted positions.

#### IV. Conclusions

Due to its great size, the [16]annulene ring has the ability to adjust its geometry easily (*i.e.*, with very small strain energy changes) in order to allow the  $\pi$  system to reach its minimum energy. The [16]annulene ring can also undergo a conformational mobility, the activation energy of which depends much more upon the resonance energy associated with the  $\pi$  system than upon strain and nonbonding energies. These facts are a great advantage for the study of the  $\pi$  system and the evaluation of the associated resonance energy, as the total number of  $\pi$  electrons is modified. We thus have investigated by spectroscopy the bond situation (bond localization or delocalization) and the geometry (planarity or nonplanarity) prevailing in the neutral [16]annulene molecule and in its radical anion and dianion, as well as the dynamic behavior of the neutral molecule and of the dianion.

According to Hückel's rule the neutral molecule should have a smaller delocalization energy than the dianion. However, as simple HMO calculations indicate, the delocalization energy should be highly positive in both species (*cf.* Table VII) and thus sufficient to force the ring to be planar. Consequently, both species R and R<sup>2-</sup> should exhibit  $\pi$ -bond delocalization and have a planar geometry. [We should note here that the Jahn-Teller theorem would not be violated if the neutral molecule would have the 85 or the 91 configuration with delocalized  $\pi$  bonds and planar geometries ( $D_{4h}$  and  $C_{2v}$  symmetry, respectively); the two nonbonding MO's are not degenerate for symmetry (*cf.* Table I); of course, the Jahn-Teller theorem does not apply to the dianion, which has the two nonbonding MO's filled.] The fact that the neutral molecule exhibits bond localization and nonplanarity in both 85 and 91 configurations implies that the delocalization energy associated with a planar 16 $\pi$ -electron system cannot be as high as predicted by simple HMO calculations. We have good reason to believe that the resonance energy of such a system is in fact negative. The argument is the following: each of the two con-

(41) J. F. M. Oth, unpublished results.

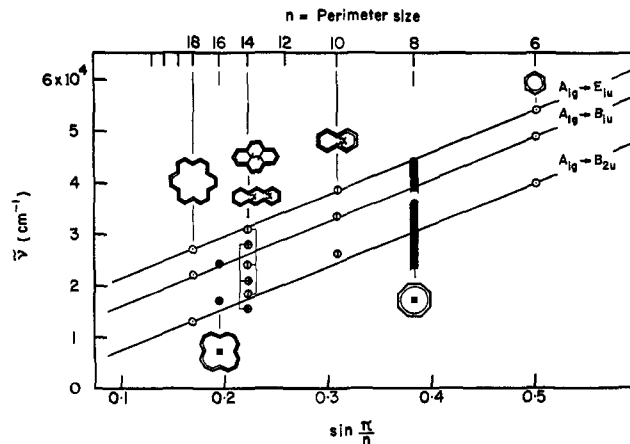


Figure 13. Position ( $\bar{\nu}$  in  $\text{cm}^{-1}$ ) of the electronic transitions observed in the "aromatic" annulenes and in the dianions of COT and of [16]annulene as a function of the size  $n$  of the perimeter.

figurations of [16]annulene undergoes an isodynamical  $\pi$ -electron shift which is characterized by a low-activation enthalpy (8  $\text{kcal mol}^{-1}$ ; *cf.* Table VII); since the transition states implied by these processes must show bond delocalization (and planarity), and since the strain energy change associated with the ring flattening is certainly smaller than 8  $\text{kcal mol}^{-1}$ , it follows that the resonance energy associated with a planar-delocalized 16-electron  $\pi$ -bond system must be slightly negative.<sup>85</sup> On the other hand, the dianion of [16]-85-annulene shows  $\pi$ -bond delocalization and is most likely planar. It also has a great thermal stability and does not show any sign of conformational mobility. These facts support the HMO prediction that the resonance energy associated with the 18 $\pi$ -electron system in the [16]annulene dianion should be  $-2\beta$  units (30  $\text{kcal mol}^{-1}$ ) greater than that associated with the 16 $\pi$ -electron system in the neutral molecule. Thus, we see that the qualitative predictions of Hückel's rule are verified here again. However, if the simple HMO calculations predict the correct order of magnitude of the difference in delocalization energy that should exist between the neutral molecule and the dianion, they do not predict their absolute values; particularly, HMO calculations do not predict that the [4 $n$ ]annulenes should have small (or even negative) resonance energies. More refined calculations, such as those made by Dewar and Gleicher,<sup>87</sup> predict those energies more correctly. Unfortunately, such calculations have not yet been made for dianions.

From the absence of any dynamic behavior in the [16]annulene dianion, and from our quantitative study of the conformational mobility shown by [18]annulene, we can conclude also that the resonance energy associated with 18  $\pi$  electrons delocalized on 16  $p_z$  atomic orbitals is greater than the resonance energy associated with 18  $\pi$  electrons delocalized on 18  $p_z$  orbitals ( $\text{DE}[16]^{2-} > 25 \text{ kcal mol}^{-1}$ ;  $\text{DE}[18] < 19 \text{ kcal mol}^{-1}$ ). This difference in delocalization energy is also predicted by simple HMO calculations.

According to simple HMO calculations, the resonance energy associated with 17  $\pi$  electrons delocalized on 16  $p_z$  atomic orbitals should be  $-\beta$  higher in energy than that of the 16 $\pi$ -electron system, and  $-\beta$  lower than that of the 18 $\pi$ -electron system. The fact that the radical anion shows bond delocalization and has a planar geometry proves that indeed it has also a

high resonance energy. The fact that the disproportionation equilibrium  $2R^{\cdot-} \rightleftharpoons R + R^{2-}$  is in favor of the radical anion indicates that the resonance energy in this species is closer to that of the dianion than that of the neutral annulene.

**Acknowledgments.** We thank Dr. P. Jung for assistance in recording the esr spectra. Our thanks are also due to Dr. L. Singer (Union Carbide Corporation, Parma Research Center) for computing the simulated esr spectra.

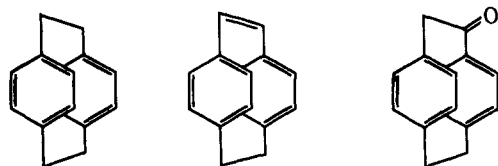
## Macro Rings. XLVI. Solvolysis with Retention of Configuration and Cis Polar Additions in the Side-Chain Chemistry of [2.2]Paracyclophane<sup>1</sup>

Robert E. Singler<sup>2</sup> and Donald J. Cram\*

Contribution No. 2812 from the Department of Chemistry,  
University of California at Los Angeles, Los Angeles, California 90024.  
Received June 28, 1971

**Abstract:** Electrophilic additions to 1,2-dehydro[2.2]paracyclophane (1) and solvolysis of resulting products were studied. Deuterium bromide addition in nonpolar solvents and bromine addition in both aprotic and protic solvents followed a cis stereochemical course. The addition products and their diastereomers underwent silver ion catalyzed acetolysis with retention of configuration. The stereochemistries of products from both the addition and solvolysis reactions were determined by a combination of nmr and chemical techniques. Conformational factors which influence assignment of configuration to one of a pair of geometric isomers are discussed. A mechanism based on the formation of highly strained phenonium ion intermediates is used to explain the stereochemical course of both the addition and solvolysis reactions.

Our previous paper demonstrated the unusual solvolytic stereochemistry and reactivity in the side-chain chemistry of [2.2]paracyclophane.<sup>2</sup> This paper reports on the stereochemical course of electrophilic additions of 1,2-dehydro[2.2]paracyclophane (1), and on the reactions of the adducts. Although the methylene bridges of [2.2]paracyclophane are in a formal sense benzylic, the uv absorption spectra of the derived olefin 1<sup>3</sup> and of 1-keto[2.2]paracyclophane<sup>4</sup> indicate that



[2.2]paracyclophane      1      1-keto[2.2]paracyclophane

the  $\pi$ -electron systems of the bridge carbons and the benzene rings are essentially unconjugated with one another. The low carbonyl absorption frequency in the infrared spectrum of the ketone ( $1698\text{ cm}^{-1}$ )<sup>4</sup> does not reflect conjugation, but rather carbonyl absorption in a large ring system.<sup>5</sup> Molecular models of [2.2]paracyclophane suggest a highly rigid structure which allows only slight deviation from face-to-face structures of the two benzene rings. Reviews of electrophilic additions<sup>6</sup> and recent investigations<sup>7</sup> indicate that both

cis and trans products occur with hydrohalide and halogen additions to olefins. The mechanisms involve cationic intermediates, and both products and rates are highly dependent on the electrophilic agent, the solvent system, added salts, and the nature of the starting olefin.<sup>7</sup> The unique geometry of 1 suggested the system might exhibit unusual stereochemical behavior in directing the course of electrophilic addition reactions. The products of addition promised to be interesting starting materials for solvolytic reactions.

### Results

**Addition of Deuterium Bromide to 1,2-Dehydro[2.2]paracyclophane (1).** Deuterium bromide in benzene-pentane at  $25^\circ$  was added to 1 to give within the limits of detection exclusively the product (48%) of cis addition, *cis*-1-bromo-2-deuterio[2.2]paracyclophane (2-*d*). In the nmr spectrum of 1-bromo[2.2]paracyclophane (2-*h*), the substituted bridge provides an ABX pattern with the highest field proton cis vicinal to the bromine on the adjacent carbon. The *cis* and *trans* coupling constants for such configurations are reported as 8.85 and 7.40 Hz, respectively.<sup>8</sup> In the 100-MHz nmr spectrum, the highest field proton band present for 2-*h* was absent for 2-*d*. In the spectrum of 2-*d*, the

(6) (a) P. B. D. de la Mare and R. Bolton, "Electrophilic Additions to Unsaturated Systems," Elsevier, New York, N. Y., 1966; (b) R. C. Fahey, *Top. Stereochem.*, **3**, 237 (1968); (c) T. G. Traylor, *Accounts Chem. Res.*, **2**, 152 (1969).

(7) (a) R. C. Fahey and H. J. Schneider, *J. Amer. Chem. Soc.*, **90**, 4429 (1968); (b) J. H. Rolston and K. Yates, *ibid.*, **91**, 1469, 1477, 1483 (1969); (c) R. C. Fahey and C. A. McPherson, *ibid.*, **91**, 3865 (1969); (d) Y. Pocker, K. D. Stevens, and J. J. Champoux, *ibid.*, **91**, 4199 (1969); (e) Y. Pocker and K. D. Stevens, *ibid.*, **91**, 4205 (1969); (f) R. C. Fahey, M. W. Monahan, and C. A. McPherson, *ibid.*, **92**, 2810 (1970); (g) R. C. Fahey and M. W. Monahan, *ibid.*, **92**, 2816 (1970).

(8) E. B. Whipple and Y. Chiang, *J. Chem. Phys.*, **40**, 713 (1964).

(1) The authors warmly thank the National Science Foundation for a grant that supported this work. Some of the results appeared in a preliminary form: R. E. Singler, R. C. Helgeson, and D. J. Cram, *J. Amer. Chem. Soc.*, **94**, 7625 (1970).

(2) R. E. Singler and D. J. Cram, *ibid.*, **93**, 4443 (1971).

(3) K. C. Dewhirst and D. J. Cram, *ibid.*, **80**, 3185 (1958).

(4) D. J. Cram and R. C. Helgeson, *ibid.*, **88**, 3515 (1966).

(5) L. J. Bellamy, "Advances in Infrared Group Frequencies," Methuen and Co., London, 1968, p 123.